SOIL MOISTURE, DEPTH OF WATER TABLE AND PEAT DECOMPOSITION IN SADONG SIMUNJAN RIVER BASIN, SARAWAK USING AIRSAR/TOPSAR DATA

[1]M. Hashim, [1]I. Busu,[1]S. H. Sim, [1]T. K. Jong, [1]W. H. Wan Kadir and [2]N. D. Salam
[1]Department of Remote Sensing, Universiti Teknologi Malaysia (UTM)
81310 Skudai, Johor Bahru, Malaysia
Tel: +607 5502969, Fax: +607 5566163, e-mail:mazlan@fksg.utm.my

[2]Soil Branch, Department of Agriculture, Kuching, Sarawak, Malaysia

ABSTRACT*:* This study reports the operational implementation of technique for the exploitation of TOPSAR data in the framework of soil condition applications. Three empirical and theoretical radar backscatter models were examined in this study to characterize radar backscatter of TOPSAR data over coastal lowland of Sadong Simunjan River Basin, Sarawak, Malaysia. The main objective of this study is to analyze relationship between radar backscatter of TOPSAR data to (i) degree of wetness of drained peatland, (ii) depth of water table and, (iii) peat decomposition. The analysis of these models were examined using varying terrain-and-sensor related parameters namely surface roughness, dielectric constant, incidence angle, polarization and frequency, respectively. These simulated backscatters were used to understand the interaction of SAR with the above three methods before mapping the soil conditions using TOPSAR data. Results of this study indicate good relationship (RMSE<5.0) exists between radar backscatters and moisture content, even in the relatively moist drained peatland, which good correlationship with the depth of water table and peat decomposition at 0.89 and 0.88 respectively.

1. INTRODUCTION

Peatland can be defined as an area where peat accumulates over time (hundreds or thousands of years) and where their formation varies at depths ranging between few centimeters to 12 meters. Peat is an organic matter formed from roots, decaying plant residue, and dead plants. The peat decomposition is very much dependent on the moisture content at which the decomposition period varies with rate of organic oxidation and reduction processes, respectively.

Completely decomposed peat will form peat substrate, and in its natural condition consists of organic-rich material (parts of plants) and water, which is very favorable for selected hardy-crops such as oil palm and pineapple. Peatland with its organic soil content is known for its importance to wetland ecology, thereby need to be preserved. However, the fertility of the decomposed organic soil have amounted pressure of being drained and converted to other uses such as agricultural or other land-related developmental projects to sustain increasing need of the local economic activities.

There has been significant research effort in the past two decades to develop remote sensing techniques to observe soil characterization from radar backscatter. Advances in active microwave remote sensing have demonstrated the ability to estimate soil moisture from

characterization radar backscatter in the surface layer under a variety of topographic and land cover conditions. In fact, several studies have demonstrated the relationship between the radar backscattering coefficient σ^o and the surface soil moisture content under varying terrain condition (Ulaby et.al, 1982; Sano et.al, 1998; Benallegue et.al, 1995).

Radar backscatter in particular Synthetic Aperture Radar (SAR) data are dependent on several nature surface parameters such as dielectric constant (Dubois et.al, 1995) and surface roughness (Evans et.al, 1992). The dielectric constant is highly dependent on soil moisture due to the large difference in dielectric constant between dry soil (typical dielectric constants of 2-3) and water (dielectric constant of approximately 80). This is formed the basis for inferring soil moisture from radar data.

Conventionally, in-situ soil moisture measurement techniques provide point measurements that do not account for the spatial variability typical of soil moisture profiles (Jackson and Schmugge, 1986). In-situ soil moisture measurements are generally expensive, often problematic, and not available at large-scale (Li et.al, 1997). Remote sensing of soil moisture may resolve these problems since it naturally provides global fields of soil moisture data at high spatial and temporal resolutions that are impractical to achieve with in-situ methods.

From the hydrological point of view soil moisture is very important parameter in the semi- and arid zones for many applications (Engman, 1991). This might be one of the main reason to the total mass of previous studies on estimating soil moisture using SAR within these regions, for example Weimann, et.al (1998) and Sano et.al (1998) to quote a few recent ones that have been mentioned previously. However, such similar studies have not been reported being undertaken in the humid tropical region, at least for the last decade in Malaysia. In fact, this rare availability is not because there are no such needs in this region or there is an existence of profound evidence to nullify that developed SAR-based moisture models are invalid in the humid tropics. But the all-weather penetration capability in SAR system, offers unrestricted constraints in acquiring remote sensing data for the tropical region like Malaysia (lies at parallel 0^o -5^o N along the Equator), which has an average of more than 75% cloud cover throughout the year (MMC, 2000)

Owing to above factors, this study is devised to examine whether or not there exist a relationship between radar backscatters with degree of wetness in Malaysia. The main focuses of this work were three folds, *i.e* to analyze relationship between radar backscatter of TOPSAR data to: (i) soil moisture (degree of wetness) (ii) depth of water table (iii) degree of decomposition of organic materials in peatland area. The water table is the level at which the water stays. It is the very top of the zone of saturation. A few centimeters above this level water can also be found due to capillary action. In the presence of a pumping well, the water table will drop around the well (Fraser, et al, 2001) and peat decomposition is level from surface, which the organic can decompose. The contents of organic compound in peatland area determine the decomposition level.

2. SCATTERING MODELS

The radar scattering models employed in study are: (a) model developed by Dubois et.al (1995) hereafter referred to as Dubois model, (b) Integrated Equation Model (IEM) Fung et.al (1992) and (c) Oh model developed by Oh et.al (1992) hereafter referred to as Oh model. Brief descriptions of these models are as follows:

2.1 Dubois Model

An empirical model describing the co-polarized backscatter coefficients of bare surface as a function of surface roughness, dielectric constant, incidence angle and frequency. The dielectric constant is the parameter sensitive to volumetric soil moisture. The hh and vv polarized backscattering cross-section σ°_{hh} (power) and σ°_{vv} (power) were empirically found by Dubois et.al (1995) to follow these two relationships:

$$\sigma^o_{hh} = 10^{-2.75}\frac{\mathrm{Cos}^{1.5}\theta}{\mathrm{Sin}\theta^5}10^{0.028\varepsilon\tan\theta}(ks\mathrm{Sin}^{1.4}\theta)\lambda^{0.7} \quad (1)$$

$$\sigma^o_{vv} = 10^{-2.35}\frac{\mathrm{Cos}^{3}\theta}{\mathrm{Sin}\theta}10^{0.046\varepsilon\tan\theta}(ks\mathrm{Sin}^{3}\theta)^{1.1}\lambda^{0.7} \quad (2)$$

where;
θ is the incidence angle (radian),
ε is the real part of the dielectric constant,
s is the root mean square (RMS) height (in cm),
k is the wave number ($k = 2\pi/\lambda$), and
λ is the wavelength (in cm)

These two relations are valid for frequencies varying between 1.5 and 11 GHz, for surfaces with roughness ranging from 0.3 to 3 cm for RMS height and for incidence angle between 30 and 60°. The backscatter coefficient σ° (units in decibel, dB), and were calculate using equation 3.

$$\text{Power} = 10^{\,dB/10} \quad (3)$$

2.2 IEM Model

This is a theoretical model, which describes the co-polarized backscatter coefficients of bare surface as a function of surfaces roughness, dielectric constant, incidence angle and frequency, and Fung et.al (1992) expressed this relationship as:

$$\sigma^o_{pp} = \frac{k^2}{2}\exp(-2k_z{}^2s^2)\sum_{n=1}^{\infty}s^{2n}\frac{|I^n_{pp}|^2}{n!}W^{(n)}(-2k_x,0) \quad (4)$$

where,

$$I_{pp}^{n} = (2k_z)^n f_{pp} \exp(-s^2 k_z^2) + \frac{(k_z)^n}{2} F_{pp} \quad (5)$$

$$f_{hh} = -\frac{2R_{\perp}}{\cos\theta} \quad \text{and,} \quad f_{vv} = \frac{2R_{\parallel}}{\cos\theta}$$

$$F_{vv} = \frac{2\sin^2\theta}{\cos\theta}\left[\left(1 - \frac{\varepsilon\cos^2\theta}{\varepsilon - \sin^2\theta}\right)(1 - R_{\parallel})^2 + \left(1 - \frac{1}{\varepsilon}\right)(1 + R_{\parallel})^2\right] \quad (6)$$

$$F_{hh} = \frac{2\sin^2\theta}{\cos\theta}\left[4R_{\perp} - \left(1 - \frac{1}{\varepsilon}\right)(1 + R_{\perp})^2\right] \quad (7)$$

$$R_{\parallel} = \frac{\varepsilon\cos\theta - \sqrt{\varepsilon - \sin^2\theta}}{\varepsilon\cos\theta + \sqrt{\varepsilon - \sin^2\theta}} \quad (8)$$

$$R_{\perp} = \frac{\cos\theta - \sqrt{\varepsilon - \sin^2\theta}}{\cos\theta + \sqrt{\varepsilon - \sin^2\theta}} \quad (9)$$

where;
pp is the polarization (hh or vv)
$R_{\parallel}$ is the *Fresnel Reflectivity* constant for vertical polarization;
$R_{\perp}$ is the *Fresnel Reflectivity* constant for horizontal polarization;
$W^{(n)}(k_x,k_y)$ is the surface roughness due power of correlation for $\rho(\zeta, \xi)$ by Fourier *transformation*:
$k_z = k\cos\theta$; $k_x = k\sin\theta$;

2.3 Oh Model

Based on empirical model, the radar backscatters are expressed in two components q and p. Both of these components are rationed of cross and hh polarisations with vv polarisation, and Oh et.al (1992) expressed them as:

$$q = \frac{\sigma_{hv}^{o}}{\sigma_{vv}^{o}} = 0.23\Gamma_{o}^{1/2}[1 - \exp(-ks)] \quad (10)$$

$$p = \frac{\sigma_{hh}^{o}}{\sigma_{vv}^{o}} = \left[1 - \left(\frac{2\theta}{\pi}\right)^{1/3\Gamma_o}.\exp(-ks)\right]^2 \quad (11)$$

where;
Γ_o is the *Fresnel Reflectivity* for surface in nadir point (see equations 10 and 11)

3. MATERIALS AND METHODS

3.1 Study Area

Fig. 1 shows the study area, located at Sadong Simunjan River Basin, Kota Samarahan of Sarawak, Malaysia covering an area of about 170 km^2 (5 by 34 km), comprising a partially drained peatland, intended for large- scale agricultural plantation. The original vegetation found here are scarce, stunted and dwindling types due to high water table and soil acidity (Lim, 1992). It is also situated in one of the largest contiguous peatland remain in Malaysia with an approximate total area of 1.6 million hectares.

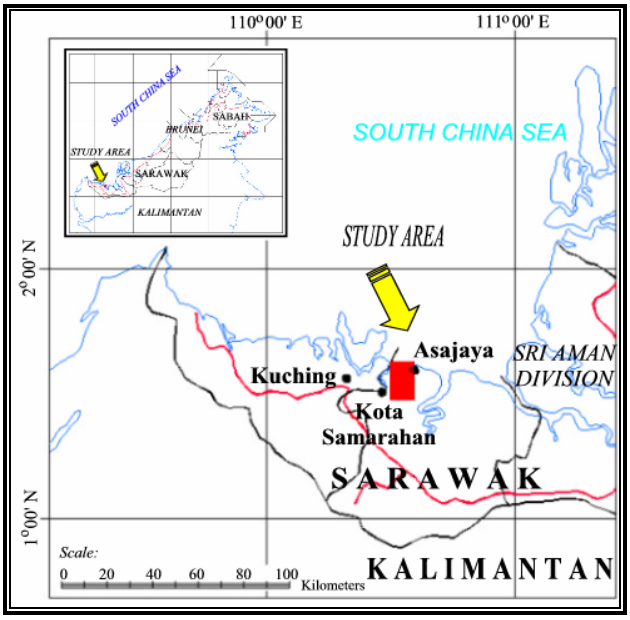

Fig 1: The study area

3.2 SAR Data

The TOPSAR data (L-band) were used in this study, acquired as part of the PACRIM I campaign, a collaborative works between Southeast Asia including Australia and New Zealand with Jet Propulsion Laboratory (JPL) /NASA of USA. The data have already been corrected for slant-to-ground range and systematically geometric corrected to local mapping datum – the Timbilai Datum of the Borneo Rectified Skew Orthomorphic Projection System. The unsystematic errors, however, have not been treated before dissemination, and were performed in this study by image-to-map registration technique. The brief technical specification of the data is tabulated in Table 1.

TABLE I.: Specification of TOPSAR Data

Parameter	AIRSAR
Band	L (1.26 GHz, 23.0 cm)
Mode	TOPSAR
Altitude	8.382 km
Incidence Angle	20° - 60°
Polarization	hh, vv and hv
Resolution	10 m x 10 m
Acquired Date	25 Nov. 1996

3.3 Ancillary Information

Remote sensing is only capable to measure the amount of radiance in their instantaneous field of view. Observation reveals that, this radiance is a mixture of different signals, one of which may be related to soil moisture. Therefore, *in-situ* ground measurements are necessary for establishing some relationship between soil moisture and observed radiance.

The ancillary information used in the study includes the topographic map of corresponding area (scale 1:50,000) and *in-situ* measurements carried out during the flight mission. Field surveys were conducted to gather samples for deriving information on the surface roughness, soil particle size, soil bulk density, and soil moisture. In addition, the depth of water table was also determined. Fig.2 shows the location of sample points collected in the study area. Two mutual sets of samples were generated, each meant for model calibration and accuracy assessments. They are designated as red and yellow ticks in Fig.2, respectively.

(i) Gravimetric Observations - the oven-drying soil moisture technique is the standard for calibration of all other methods. The method involves obtaining a wet soil sample weight, W_w drying the sample at 100°C for 24 hours, and then obtaining the dry sample weight W_d. Then with a measurement of the bulk density, Y_d and the density of water, Y_w the volumetric water content can be found:

$$M_v = \frac{W_w Y_d}{W_d Y_w} 100\% \qquad (12)$$

(ii) Soil Roughness Measurements – The height profiles of the soil surface were measured by a 1.5-meter made of a raw of 100 pins, spaced 1 centimeter for 1 meter and 100 pins spaced 0.5 cm for 0.5 meter. The relative pin elevations are recorded photographically, after which they are digitized with AutoCAD software and analyzed to obtain surface profiles. From these measurements, three parameters can be calculated: standard deviation of surface height; correlation length and standard deviation of surface height slope (Table II and Table III). The design of these profilometer is based on Hoekman et.al (2000).

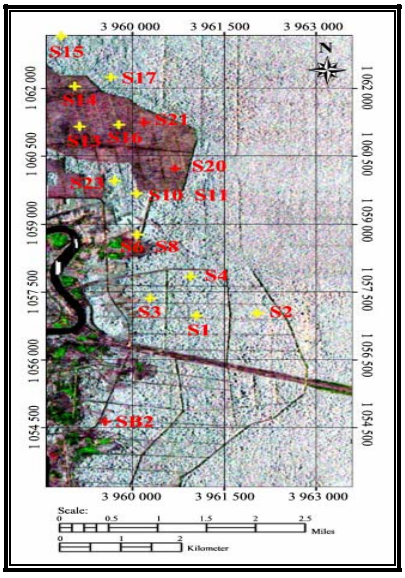

Fig 2: Location of sampling points

TABLE II. Volumetric Soil Moisture and Soil Roughness for the Sample Calibrating Radar Backscattering Models

ID Point	Surface Roughness (s, cm)	Correlation Length (ℓ, cm)	Soil moisture (M_v, vol)
S1	3.080	11.864	0.71
S2	2.994	13.845	0.87
S3	0.935	2.696	0.76
S4	1.463	7.690	0.69
S8	0.333	31.589	0.53
S10	1.511	33.166	0.72
S11	2.000	31.208	0.64
S13	0.445	28.496	0.68
S14	1.037	28.980	0.62
S15	1.746	23.754	0.70
S16	1.580	31.946	0.63
S17	2.327	24.377	0.75
S23	2.310	27.039	0.78

TABLE III. Check Points Used for Accuracy Analysis of Volumetric Soil Moisture and Soil Roughness for the Check Points

ID Point	Surface Roughness (s, cm)	Correlation Length (ℓ, cm)	Soil moisture (M_v, vol)
S6	0.706	29.875	0.63
S20	2.318	32.067	0.80
S21	2.283	27.105	0.70
S22	2.338	27.229	0.80
SB2	2.317	12.137	0.61

3.4 Data Processing

3.4.1 Speckle Reduction

Speckles found in SAR data due to random multiplicative noise, can be recognized by the random pattern and the noise levels increases with average gray level of specified window area in an image scene (Lee, 1986). Minimization of speckle effects in SAR data were carried out using adaptive radar filter (Lopes et.al, 1990). In this study, several radar adaptive filters and convolution filters were used, namely Lee, Frost, Gamma, Kuan, Local-Sigma, Low- Pass, Laplacian, Gaussian and Median. Results in this study indicates that Gaussian 7x7 filter is the best for this area, reporting best coefficient of variance test (Paudyal and Aschbacter,1993). Furthermore, the windows size 7 x 7 was also within reasonable spatial variations of the target of interest at the spatial resolution of the TOPSAR data.

3.4.2 Extraction of Surface Roughness and Soil Moisture

The main core processing carried out in this study was to extract surface roughness and soil moisture from radar backscatters of the TOPSAR data. In the first task, the surface roughness (s) or the RMS heights were computed using all the three backscatter models employing equations (1) and (2) for Dubois model; and equations (10) and (11) for Oh model. In the case of IEM model, which involves by rigorous computation, a computer program developed by Fung et.al (1992) were used. Apart from computed surface roughness (s), the same parameter was computed directly using TOPSAR data after it was preprocessed and converted into dB image. This is then known as s computation directly from image.

In the second processing task, the soil moisture estimation was performed using the regression analysis approach with main input derived from radar backscatters parameters obtained in the first task other than using image direct.

3.4.2.1 Dielectric Constant

For the selected models examined the critical input is the dielectric constant ε. In this study approach by Hallikainen, et.al (1985) has been adopted, where dielectric constant measurements for five different soil types at frequencies between 1.4 and 18 GHz were established. Based on these measurements, polynomial expressions can be derived relating the real and imaginary part of ε to the volumetric moisture content, Mv, and the percentage of sand and clay. These polynomial expressions are of the following form:

$$\varepsilon = (a_0 + a_1 S + a_2 C) + (b_0 + b_1 S + b_2 C) Mv + (c_0 + c_1 S + c_2 C) Mv \qquad (13)$$

where;
S is the percentage (by weight) of sand,
C is percentage of clay, and
a_i, b_i, c_i are coefficients, which depend on frequency.

3.4.1 Extraction of Depth of Water Table

Depth of water table (DWT) is main factor to decide what type of crop to plant in converted peatland. Strong relationship existence between plants type and DWT, which also influence roots for water uptake (Melling et.al, 1999). In this study, the water depth for each ID point was determine with measure from ground surface that the level which the water stays around a well.

For determine the correlation between water depth information and backscatter value extracted from TOPSAR data, regression technique was employed. Multiple linear regressions were generated for both information and correlation coefficient (R^2) given shows correlation for each point. Table IV shows DWT information during sampling on 21 till 23 July 1999 over Sadong Simunjan River Basin, Sarawak.

Table IV: Water Depth Information on Sampling Site

ID point	Coordinate (m)		Water depth (m)	ID point	Coordinate (m)		Water depth (m)
	Easting	Northing			Easting	Northing	
S1	3960230	1056345	-0.750	S25	3960061	1058800	-0.640
S2	3959928	1057398	-0.400	S26	3959766	1058898	-0.300
S3	3960482	1056210	-0.300	S27	3960015	1059234	-0.400
S4	3960935	1056177	-1.500	S28	3959989	1059797	-0.320
S5	3960297	1056861	-0.310	S29	3959283	1060839	-0.500
S6	3960423	1057107	-0.010	S30	3959019	1062163	-0.330
S7	3960305	1057222	-0.190	S31	3959624	1062245	-0.360
S8	3960364	1057291	-0.350	S32	3959941	1061278	-0.340
S9	3960237	1057323	-0.320	S33	3960567	1061137	-0.300
S10	3960012	1057370	-0.360	S34	3959637	1061073	-1.500
S11	3960440	1057367	-0.470	S35	3961058	1060241	-0.500
S12	3960627	1057416	-0.400	S36	3959449	1059865	-0.200
S13	3960888	1057399	-0.100	S37	3959501	1059976	-0.250
S14	3961063	1057379	-0.550	S38	3959645	1060098	-0.260
S15	3961014	1057591	-0.050	S39	3959713	1060047	-0.700
S16	3960330	1057521	-0.340	S40	3959807	1060003	-0.350
S17	3960267	1057427	-0.250	S41	3961535	1058130	-0.320
S18	3960464	1057600	-0.200	S42	3962624	1058199	-0.200
S19	3960472	1057625	-0.220	S43	3963016	1057390	-0.300
S20	3960086	1057688	-0.230	S44	3963410	1056089	-0.050
S21	3960844	1058086	-0.130	S45	3962038	1056642	-0.100
S22	3960278	1058087	-0.700	S46	3960993	1056760	-0.220
S23	3960357	1058615	-0.150	S47	3961879	1057391	-0.150
S24	3960009	1058725	-0.430	S48	3961001	1058398	-0.680

3.4.2 Extraction of Degree of Peat Decomposition

Determinations of decompose level of organic matter of peatland area. Commonly, peatland can divided to three parts (Lim, 1992) and presented as (i) sapric, (ii) hemic, and (iii) fibric. The composition of standard peatland is comprised 80 percent of organic matter and the ratio can be calculate from this equation:

$$\text{Organic matter (\%)} = 100 - (\text{\% ash} + \text{\% water}) \quad (16)$$

Based on equation 16, mass of water contents is input parameter to determine a organic matter. Table V shown a peatland water contents during a sampling period.

TABLE V. Peatland Water Contents from Samples

Point ID	*W1=Land + Ring*	*W2=Land + ring $_{dried}$*	*W3 = ring weight*	*W4 = W2-W3 $Mass_{Dry\ Soil}$*	*W1=W2 $Mass_{Water}$*	*$Mass_{water\ content}$ (W1-W2) x100/W*
S1	185.20	114.66	96.35	18.31	70.54	385.25
S2	201.23	114.24	99.77	14.47	86.99	601.17
S3	193.44	117.50	97.67	19.83	75.94	382.96
S4	183.32	114.80	96.79	18.01	65.52	380.46
S5	184.85	114.08	98.07	16.01	70.77	442.04
S6	240.31	177.77	100.38	77.39	62.54	80.81
S7	227.26	166.76	92.78	73.98	60.50	81.78
S8	237.58	184.31	96.77	87.54	53.27	60.85
S9	240.61	186.32	90.78	95.54	54.29	56.82
S10	192.04	119.72	97.48	22.24	72.32	325.18
S11	194.20	130.57	95.90	34.67	63.63	183.53
S12	198.44	126.17	97.61	28.56	72.27	253.05
S13	196.06	127.81	93.32	34.49	68.25	197.88
S14	215.89	153.58	97.85	55.73	62.31	111.81
S15	178.65	108.90	94.96	13.94	69.75	500.36
S16	189.22	125.99	97.84	28.15	63.23	224.62
S17	193.71	118.70	94.79	23.91	75.01	313.72
S18	184.09	114.81	97.66	17.15	69.28	403.97
S19	195.86	118.35	95.93	22.42	77.51	345.72
S20	196.56	116.21	99.21	17.00	80.35	472.65
S21	187.26	116.86	97.45	19.41	70.40	362.70
S22	192.76	112.53	95.72	16.81	80.23	477.28
S23	191.02	113.13	93.43	19.70	77.89	395.38
S24	192.89	112.20	97.56	14.64	80.69	551.16
S25	249.67	193.16	96.95	96.21	56.51	58.74

4. RESULTS AND DISCUSSION

The derived surface roughness (s) from the respective models was compared with Mv obtained from in-situ measurements with regression analysis, and their respective relationship (based on r^2) are summarized in Table VI.

TABLE VI: Summary of Results of Regression Analysis Carried Out.

Relationship analyzed	Image Direct$^{\Psi}$		Dubois Model		IEM Model		Oh Model	
	L_{hh}	L_{vv}	L_{hh}	L_{vv}	L_{hh}	L_{vv}	L_{hh}	L_{vv}
Mv vs σ°	0.53	0.38	0.76	0.89	0.54	0.54	0.57	0.34
s vs σ°	0.37	0.46	0.82	0.69	0.75	0.70	0.49	0.97
θ vs σ°	0.21	0.42	0.21	0.28	0.39	0.45	0.22	0.14

Note: $^{\Psi}$ Refer to TOPSAR data

4.1 Soil Moisture

With regard to the Mv versus backscattering coefficients, the best relationship found with Dubois model with r^2 =0.8 and 0.9 in hh and vv polarizations, respectively. Fig. 3 and Fig. 4 exhibit these relationships and the best-fit models are given by equation 13 and 14. The other models: Oh and IEM, however, do not show any significance when compared to original backscatters derived from image direct. This is evident with relatively the same r^2 shown by these models against image direct.

hh-Polarization: $M_v = 0.610\sigma_{hh} + 45.99$ (13)

vv-Polarization: $M_v = 0.765\sigma_{vv} - 49.93$ (14)

The relationship of s and radar backscatters (σ°) was reported best with Dubois model (r^2 =0.8) followed by IEM model (r^2 =0.7), both in the hh polarizations. This shows most other models is a weak relationship between incidence angle and backscatters, this is also exhibited by the r^2 in range of 0.1 to 0.4. Of all the models analyzed, Oh model was found to be most inferior whilst s and Mv are the best correlated by Dubois model. IEM model fits in between Dubois and Oh models.

Next, the Mv and s derived from the respective models were also analyzed for root mean square error (RMSE). This was achieved by comparison of the respective values with the corresponding in-situ measurements (the mutual test set), and the results obtained are summarized in Table VII. Again Dubois model shows the best result, with Mv best be determined with L_{hh} whilst the s with L_{vv}. The RMSE obtained here are comparable to the results obtained by Dubois et.al (1995), around 4.2 percents.

TABLE VII: Summary of RMSE of model examined

	Image Direct$^{\Psi}$		Dubois Model		IEM Model		Oh Model$^{\tau}$	
	L_{hh}	L_{vv}	L_{hh}	L_{vv}	L_{hh}	L_{vv}	L_{hh}	L_{vv}
Mv	7.97	9.74	4.41	3.25	8.27	8.59	-	-
s	0.80	1.27	0.37	0.48	0.43	0.50	-	-

Note: $^{\Psi}$ Refer to TOPSAR data
$^{\tau}$ most inferior to count

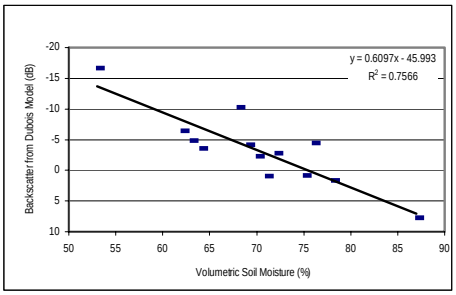

Fig.3. Estimated $\sigma°L_{hh}$ calculated from Dubois model versus Mv

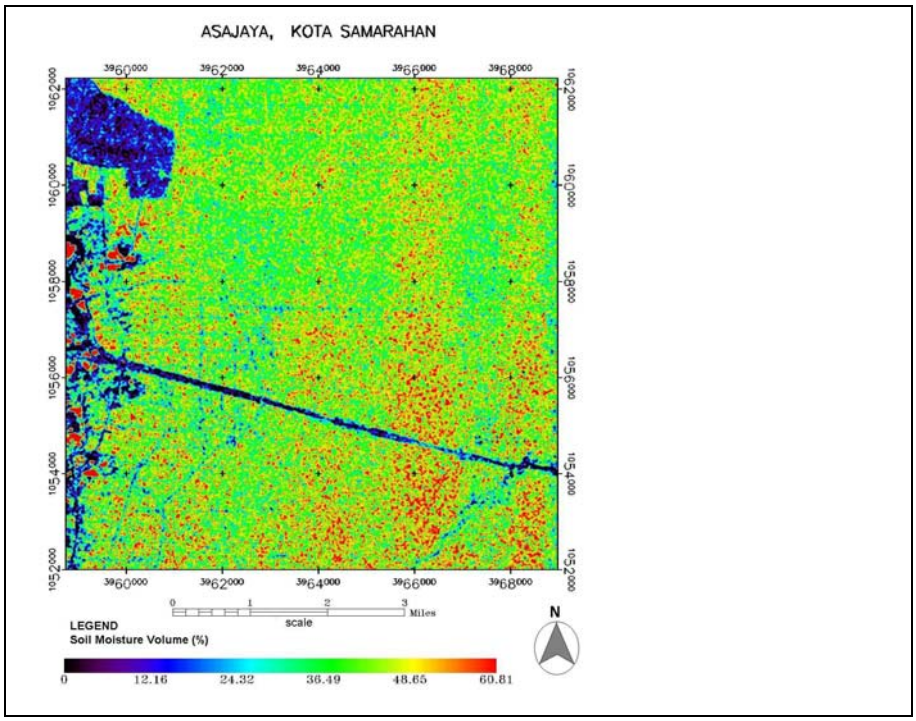

Fig 4. Mv map derived from TOPSAR L_{hh} using Dubois model

4.2. Depth of Water Table

Depth of water table (DWT) may be defined above ground level. Information of DWT is vital parameter in this study. Only 23 points were used to generate the fitted model this information can relate of each backscatter value due to water depth and its can explain in equation 15.

The regression model was generated using all of the specified independent variables, the best fit model of DWT is:

$$DWT = 1.969 + 0.003\sigma^{o}_{Lhh} + 0.045\sigma^{o}_{Lvv} + 0.056\sigma^{o}_{Lhv} + 0.035\sigma^{o}_{Phh} + 0.006\sigma^{o}_{Pvv} + 0.017\sigma^{o}_{Phv} \quad (15)$$

where:

σ°_{Lhh}, $\sigma^{\circ}_{Lvv}\sigma^{\circ}_{Lhv}$, σ°_{Phh}, σ°_{Pvv}, σ°_{Phv} are backscatter value from co-polarized TOPSAR image.

The P-value gives the probability of getting a value of t with absolute value greater than that observed if the null hypothesis H_0 is true. The statistical test carried out such that hypothesis tested are H_0 is coefficient equal 0 and H_A coefficient not equal 0. If the P-value falls below 0.05, the null hypothesis is rejected at the 5 percent significance level. In such case, the coefficient corresponding to L_{hv} are statiscally significant, while other variables

are found insignificant. The water depth table map was derived using best fit model (equation 15) is shown in **Fig. 5**. The areas near riverbanks were found having a higher water depth compare with inland area. Comparing with 'ground truth'- 25 check points were used for assessing the accuracy of model generated, and the results is summarized in Table VII.

Table VIII: Summary Results from Multiple Linear Regression for Water Depth Analysis

Parameter	Estimate	Standard Error	t-statistic	P-value
Variables	1.969	0.8226	2.39	0.0621
L_{hh}	0.003	0.0247	0.10	0.9211
L_{vv}	0.045	0.0413	0.109	0.3238
L_{hv}	0.056	0.0306	1.83	0.1262
P_{hh}	0.035	0.0329	1.05	0.3406
P_{vv}	0.006	0.0189	0.30	0.7748
P_{hv}	0.017	0.0379	0.44	0.6790
Correlation Coeff. R^2				0.89
Std. Dev. (Estimation)				0.201147
Average Deviation (Absolute)				0.106759
Confidence Level				95%

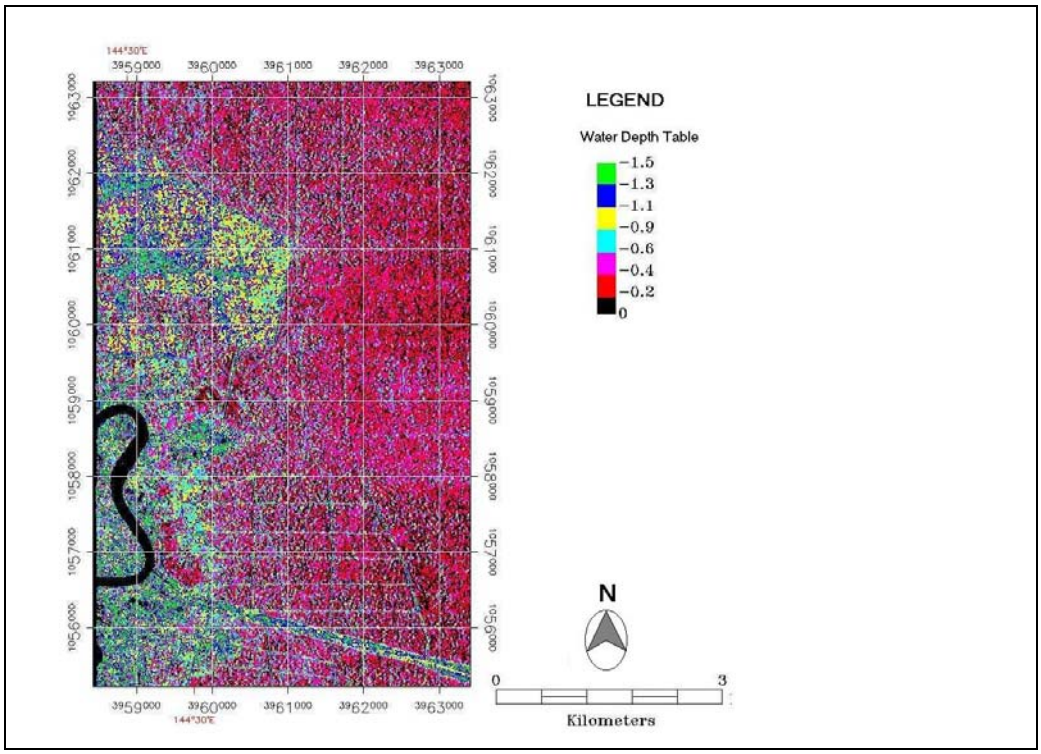

Fig 5: Depth of water table over study area using L band and P band

4.3 Peatland Decomposition

Peat decomposition level can be determined using three common methods, namely: (i) bulk density (ii) pyrophosphate color test, and (iii) fibre contents. In this study, only determination bulk density peat was adopted

.

$$\text{Bulk density} = \frac{Mass\,(\text{g})}{\text{Vol}\,(\text{cm}^3)} \qquad (17)$$

Table IX. Multiple Regression of Bulk Density.

Parameter	Estimate	Standard Error	t-statistic	P-value
Variables	0.6849	0.7924	0.86	0.4510
L_{hh}	-0.0202	0.0173	-1.17	0.3270
L_{vv}	-0.0484	0.0318	-1.52	0.2258
L_{hv}	-0.0448	0.0228	-1.96	0.1446
P_{hh}	0.0662	0.0335	-1.98	0.1426
P_{vv}	-0.0740	0.0242	-3.06	0.0551
P_{hv}	0.0632	0.0354	-1.79	0.1719
Correlation Coeff. (R^2)				0.88
Coeff of Variation				46.80%
Average Deviation (Absolute)				0.0590
Average Deviation (Estimation)				0.1384
Confidence Level				95%

The fit model for bulk density determined from backscatter of TOPSAR data is best given by equation 18 with $r^2 = 0.8$.

$$\begin{aligned} \textit{Bulk Density} = 0.6849 - -0.0202\sigma^{o}{}_{Lhh} - -0.0484\sigma^{o}{}_{Lvv} + 0.0561\sigma^{o}{}_{Lhv} - \\ - 0.0448\sigma^{o}{}_{Phh} + 0.0662\sigma^{o}{}_{Pvv} - -0.0740\sigma^{o}{}_{Phv} \end{aligned} \qquad (18)$$

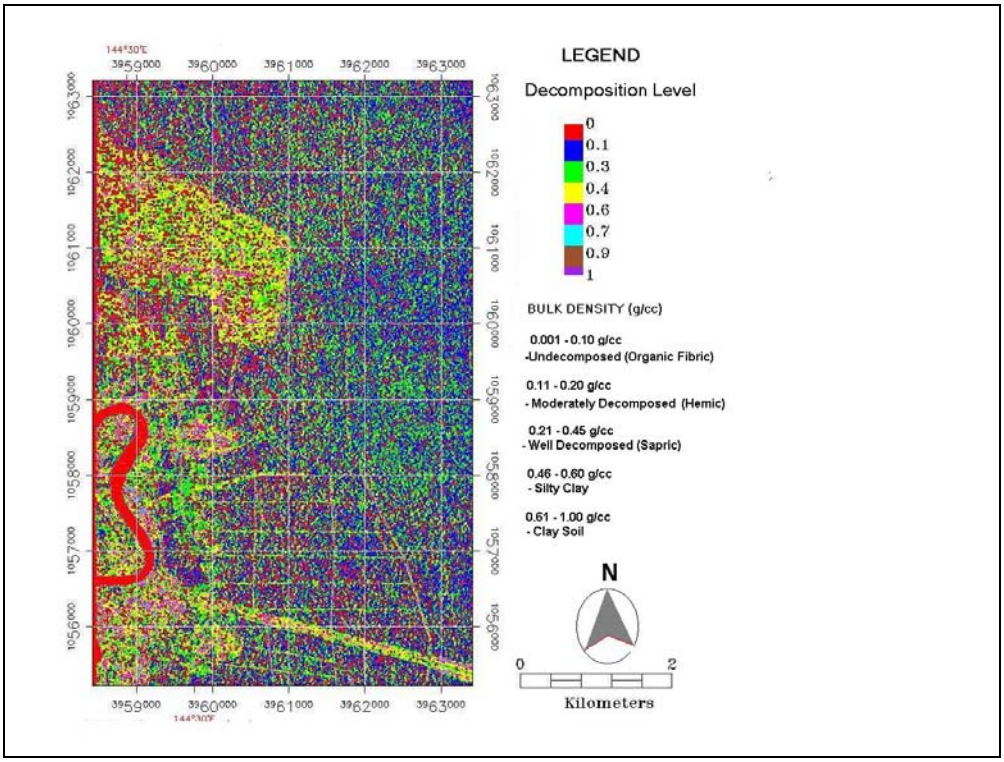

Fig. 8: Decomposition level of peatland area.

5. CONCLUSIONS

The results presented in this study have demonstrates that soil moisture, depth of water table and degree of decomposition within peatland can be estimated using TOPSAR data. Of all the radar backscattering models examined, Dubois model is the best for TOPSAR data for all three parameter tested. The soil moisture and surface roughness is best estimated using L_{hh} and L_{vv} co-polarized TOPSAR which is more sensitive to degree of wetness in the tropical region. With regard to depth of water table and peat decomposition, co-polarized L and P bands can adequately be modeled for extraction of these parameters with correlation of above 80 percent. It is anticipated with liner spatial resolution of polarized multi band SAR would enhance all the results obtained in this study in near future, where multipolarized SAR band are planned for adequate earth observation.

REFRENCES

Benallegue, M., O. Taconet, D. Vidal-Madjar, and M. Normand, "The Use of Radar Backscattering Signals for Measuring Soil Moisture and Surface Roughness." Remote Sensing of Environment, Vol.53. 61-68, 1995

Dubois, P. C., J. V. Zyl, and E. T. Engman, "Measuring Soil Moisture with Imaging Radars." IEEE Transactions on Geoscience and Remote Sensing, Vol. GE-33(4). 915-926. 1995

Engman, E. T. "Applications of Microwave Remote Sensing of Soil Moisture for Water Resources and Agriculture." Remote Sensing of Environment, Vol. 35.213-226, 1991

Evans, D. L., T. G. Farr, M. Vogt, C. Bruegge, J. Conel, R. E. Arvidson, S. Petroy, J. J. Plaut, M. Dale-Bannister, E. Guinness, R. Greeley, N. Lancaster, L. Gaddis, J. Garvin, D. Deering, J. R. Irons, F. Kruse and D. J. Harding. "The Geologic Remote Sensing Field Experiment." IEEE Transactions on Geoscience and Remote Sensing. 1992

Fraser, C. J. D., Roulet, N. T. Lafleur, M. "Groundwater flow patterns in a large peatland" Jounal of Hydrology. Vol 246; 142-154, 2001

Fung, A. K. Z. Li, and K. S. Chan, "Backscterring from a Radomly Rough Dielectric Surface." IEEE Transactions on Geoscience and Remote Sensing. Vol. GE-30(2). 356-369, 1992

Hallikainen, M. T., F. T.Ulaby, M. C. Dobson, M. A. El-Rayes, and L. K. Wu, "Microwave Dielectric Behavior of Wet Soil – Part1: Empirical Models and Experimental Observations." IEEE Transactions on Geoscience and Remote Sensing, Vol. GE-23(1). 25-34, 1985.

Hoekman, D. H., L. Woodhouse and P. V. Oevelan, "Validation of Backscatter Model for Interpretation of Microwave Signature in Term of Structure and Vegetation Characteristic of Boreal Forest (No. 8).
URL: http://hydserver.hyd.uu.se/nepex/explan2/spp88.html

Jackson, T. J., and T. J. Schmugge, "Passive Microwave Remote Sensing of Soil Moisture." in. Chow, V. T.. "Advances in Hydroscience." London: Academic Press Inc. Ltd.. 123-157. 1986

Lee, J. S. "Speckle Suppression and Analysis for Synthetic Aperture Radar Images." Optical Engineering, Vol. 25(5). 636-643, 1986

Li, K. Y., R. D. Jong, and J. B. Boisvert, "Estimating Soil Moisture Profiles in the Root Zone Using Intermittent Remotely Sensed Surface Moisture Contents." International Symposium Geomatics In The Era of Radarsat, GER '97. 2nd Edition. Ottawa, Canada. [CD-ROM], 1997.

Lim, E. T. "Peat Soil of Sarawak and Their Methods." Chemistry Division Agriculture Research Centre, Department of Agriculture, Sarawak, 1992

Lopes, A., R.Touzi and E. Nezry, "Adaptive Filters and Scene Heterogeneity." IEEE Transactions on Geoscience and Remote Sensing. Vol. GE-28(6). 992-1000, 1990.

Melling, L., Ambak, K., Osman J and Husni, A. "Water Management for the Sustainable UtIlization of Peat Soils for Agriculture." A paper presented at the *International Conference and Workshop on Tropikal Peat Swamps*: Sage guarding a global natural natural resource. Penang, Malaysia. 22 – 29, July, 1999

MMC, Malaysia Meteorological Service Report "Climate of Malaysia"., 2000.

Oh, Y., K. Sarabandi and F. T. Ulaby, "An Emprical Model and An Iversion Technique for Radar Scattering from Bare Soil Surfaces." IEEE Transactions on Geoscience and Remote Sensing. Vol. GE-30(2). 370-381, 1992.

Paudyal D. R., and J. Aschbacter, "Evaluation and Performance Test of Selected SAR Speckles Filter." The International Symposium Operationallization Org. Remote Sensing." ITC Enschede, Nertherland, 1993.

Sano, E. E., M. S. Moran, A. R. Huete, and T. Miura, "C-and Multiangle Ku-Band Synthetic Aperture Radar Data for Bare Soil Moisture Estimation In Agricultural Areas." Remote Sensing of Environment, Vol.64. 77-90, 1998.

Ulaby, F. T., A. Aslam, M. C.Dobson, "Effects of Vegetation Cover on the Radar Sensitivity to Soil Moisture", IEEE Transactions on Geoscience and Remote Sensing, Vol. GE-20(4). 476-481. 1982a.

Weimann, A., M. V. Schonermark, A. Schumann, P. Jorn, and R. Gunther, "Soil Moisture Estimation with ERS-1 SAR Data In The East-German." International Journal of Remote Sensing. Vol. 19(2). 237-243, 1998.